

Interaction of ZIF-8 with Cu²⁺ in water solutions for remediation applications

L. G. Barbata,^a E. Sangiorgi,^a M. M. Calvino,^a F. Armetta,^{b,c} G. Lazzara,^a M. L. Saladino,^{b,c} M.

Scopelliti,^a F. M. Gelardi,^a S. Agnello,^{a,d} and G. Buscarino^a

^a Dipartimento di Fisica e Chimica - Emilio Segrè, Università di Palermo, Viale delle Scienze
Ed.17, I-90128 Palermo, Italy

^b Dipartimento Scienze e Tecnologie Biologiche, Chimiche e Farmaceutiche – STEBICEF,
Università di Palermo, Viale delle Scienze Ed.17, I-90128 Palermo, Italy

^c CNR—Istituto per i Processi Chimico Fisici, Viale Ferdinando Stagno D'Alcontres 37, 98158
Messina, Italy

^d ATEN Center, University of Palermo, Viale delle Scienze Ed. 18, 90128, Palermo, Italy

Corresponding author: gianpiero.buscarino@unipa.it

Interaction of ZIF-8 with Cu²⁺ in water solutions for remediation applications

L. G. Barbata,^a E. Sangiorgi,^a M. M. Calvino,^a F. Armetta,^{b,c} G. Lazzara,^a M. L. Saladino,^{b,c} M. Scopelliti,^a F. M. Gelardi,^a S. Agnello,^{a,d} and G. Buscarino^a

^a Dipartimento di Fisica e Chimica - Emilio Segrè, Università di Palermo, Via Archirafi, 36, I-90123 Palermo, Italy

^b Dipartimento Scienze e Tecnologie Biologiche, Chimiche e Farmaceutiche – STEBICEF, Università di Palermo, Viale delle Scienze Ed.17, I-90128 Palermo, Italy

^c CNR—Istituto per i Processi Chimico Fisici, Viale Ferdinando Stagno D'Alcontres 37, 98158 Messina, Italy

^d ATEN Center, University of Palermo, Viale delle Scienze Ed. 18, 90128, Palermo, Italy

Corresponding author: gianpiero.buscarino@unipa.it

Abstract

Water pollution is a global environmental problem and now more topical than ever. Among several pollutants, heavy metals are of particular interest due to their toxicity and high bioaccumulation capacity. Metal-organic frameworks (MOFs) are exceptional adsorbents for capturing metal ions in water. Between them, ZIF-8 has high sequestration capacity of copper ions in water, but the capture mechanism remains unclear. The scope of this work is to investigate the interaction of ZIF-8 with copper ions in aqueous solution at pH=7, discriminating between effects due to water, copper and those resulting from their concomitant presence. Several samples were prepared dispersing a certain amount of ZIF-8 in an aqueous Cu²⁺ solution at a fixed concentration in the range between 0-300 mg/L. X-ray diffraction, Raman Spectroscopy, gas porosimetry, Thermogravimetry, X-ray photoelectron spectroscopy (XPS) and Electron Paramagnetic Resonance (EPR) were used to evaluate the structural features of the ZIF-8 before and after Cu²⁺ capture. Our results indicates that

ZIF-8 is capable to capture high amounts of Cu^{2+} , but in aqueous solution it undergoes a dissolution and reorganization process that affect its applications in simply powder form.

Keywords: ZIF-8, water remediation, MOF

1. Introduction

Access to safe drinking water is one of the hot topics of recent decades and one of the greatest challenges to be faced today. In fact, of all the water available on the planet, only 3% is suitable for human use and today more than 1.2 billion people do not have access to drinking water^{1,2}.

The increasing development of industrial plants, mining, energy, and agriculture or, in any case, any anthropogenic activity contributes to the increase of toxic substances and pollutants dispersed into the environment and water during production processes, with the consequence of increasingly reducing the possibility of access to clean water^{3,4}. Between the various different water pollutants, heavy metals pose one of the greatest dangers because these elements are widely recognised as bioaccumulative, i.e. they are unlikely to be eliminated from the body once introduced so their effects are not immediately visible and are responsible for severe human pathologies⁵. Copper is one the metals that play a role in normal biological human activity when is assumed within the recommended daily intake, fixed by OMS and FDA at ~ 1 mg/day, but in higher quantities it is toxic to human health^{6,7,8}. Copper accumulation is frequently found due to its wide use as a fungicide in agriculture^{9,10}. High copper concentrations can often lead to gastrointestinal disorders, stomatitis, and haemoglobinuria, which are hardly diagnosed as side effects of heavy metal intoxication^{11,12}. Hence it is clear, for the reasons stated above, that water pollution by heavy metals is a rising environmental issue, and therefore new methodologies and materials are currently being researched and developed for efficient water remediation. Metal-organic frameworks (MOFs) are promising materials for water remediations, they are composed of metal ions coordinated by organic linkers which arrange together in crystalline structures¹³. MOFs possess very high surface area making them capable to capture high

amounts of pollutants and moreover are very versatile because their structure could be tailored for its own needs making them highly selective toward the species to capture^{14,15}. In order to be able to use MOFs as adsorbents, one aspect not to be neglected is their stability in water because they may undergo hydrolysis processes. For these reasons, Zeolitic Imidazolate Frameworks, especially ZIF-8, are gaining a rising interest in the field of water remediation. ZIF-8 is a MOF, composed of Zn²⁺ and the organic linker 2-methylimidazole (2-MeIm), that since its first appearance by Park *et al.*¹⁶ was reported to be highly stable also in extreme conditions like boiling water, methanol, benzene and alkaline solution where it retained its crystalline structure after 7 days of treatment in these conditions. However, more recent findings^{17,18} have shown that ZIF-8 is not so stable in water as previously reported, because when it is exposed to water solutions, with a ZIF-8/water weight ratio of 6.0 wt.% or lower, a formation of a new unknown dense and non porous crystalline phase is observed simultaneously to the loss of crystallinity of the residual ZIF-8. These results suggest that ZIF-8 structure undergoes to a hydrolysis reaction that involves the Zn-N bonds. Despite this, many different applications in water remediation of ZIF-8 are reported, in detail regarding heavy metal adsorption^{19,20,21} showing the outstanding results obtained for Cu²⁺. Zhang *et al.*²² reported a study about the absorption of copper ions on ZIF-8 in water solution at pH=4, in a concentration range of 2-420 mg/L of Cu²⁺, showing that the Cu²⁺ amount adsorbed per unit mass of ZIF-8 grows monotonically as the initial concentration of the metal in solution increases, until it reaches values of about 800 mg/g that is much higher than any other material used for Cu²⁺ removal. Measurements of Inductively coupled plasma mass spectrometry (ICP-MS) have shown that Zn²⁺ is gradually released in solution as Cu²⁺ concentration rises till a threshold value of 200 mg/L of Cu²⁺, beyond which concentration of released Zn²⁺ remains constant. However, the absorption mechanism remains unclear because for concentration of copper ions till 200 mg/L an ionic exchange between copper and zinc seems to happen in the structure of ZIF-8, but for higher concentrations of copper X-ray Diffraction (XRD) and Transmission Electron Microscopy (TEM) data have shown that the material undergoes to a complete loss of its crystalline structure. Also, in the study of Zhang *et al.*²² the effect

of water alone on the structure of ZIF-8 was not considered although the ZIF-8/water weight ratio used is the one where hydrolysis is expected to occur, and tests were carried out at pH=4 which is an unusual value for freshwater.

Moreover, Zhang *et al.*²³ investigated the effect of different metal salts water solutions on ZIF-8 structure. The results obtained from XRD and Porosimetry indicate that univalent cations have no effects on ZIF-8 structure but bivalent and higher cations destroy the crystalline ZIF-8 structure and the effect is more considerable with increasing the concentration of cations or their valence. Indeed, the diameters of bivalent and trivalent cations (0.78-2.04 Å) are smaller than the window of ZIF-8 (3.4 Å), so they can diffuse into the cages of ZIF-8 to contact any imidazolate anions. If the imidazolate anion has a stronger interaction with a cation than with Zn²⁺, the cation should be able to substitute Zn²⁺, leading to the collapse of ZIF-8 structure and this explanation was confirmed by the authors with DFT calculations which show that the substitution of Zn²⁺ with some bivalent and trivalent cations is energetically favourable²³.

It is clear that the debate on the stability of ZIF-8 in water and its applicability for water remediation from heavy metal ions is still open. Therefore, this study aims to investigate the interaction between ZIF-8 and copper ions in aqueous solutions at pH=7 in a concentration range of 0-300mg/L of Cu²⁺, to clarify issues that are still poorly understood in the literature and to assess the possibility of practically using ZIF-8 as a water purification system. Moreover, possible negative consequences of ZIF-8 treatment, such as the possible degradation of the material structure and any secondary pollution resulting from it, were also be considered. For this purpose, different experimental techniques such as Electron Paramagnetic Resonance (EPR), Raman spectroscopy, XRD, porosimetry, X-ray photoelectron spectroscopy (XPS) and Thermogravimetry (TGA) were employed.

2. Materials and Methods

ZIF-8 used in this work is in powder form, purchased by Sigma-Aldrich (Basolite Z1200). $\text{Cu}(\text{NO}_3)_2 \cdot 3\text{H}_2\text{O}$ was of analytical grade and acquired by Sigma-Aldrich. Milli-Q water ($18.2 \text{ M}\Omega \text{ cm}^{-1}$, $\text{pH}=7$) was used throughout the experiments.

Several samples were prepared by the following procedure: 100mg of ZIF-8 were dispersed by sonication in 100mL distilled water solutions of $\text{Cu}(\text{NO}_3)_2 \cdot 3\text{H}_2\text{O}$ with concentrations of 0, 50, 100, 150, 200 e 300 mg/L. The reference sample with 0 mg/L of Cu^{2+} was prepared to evaluate the effect of only water exposure and was labelled as **ZIF-8+H₂O**. The dispersions were left stirring for 30min and then the solids were recovered by vacuum filtration. At this point two different sets of samples were obtained: one set was dried at room temperature while the second set was dried at 70° C in an oven. The two set of samples are labelled as **Room temperature** and **Oven 70 °C** respectively.

XRD patterns were acquired through a Rigaku MiniFlex diffractometer using Cu K α radiation source, in a 2θ range between 5° and 40°, with a scanning speed of 5°/min and in steps of 0.02°.

Raman measurements were performed at room temperature and using the Horiba LabRAM HR-Evolution Raman spectrometer using 25% and 50% ND filters and 50×LWD objective, acquisition time of 15 s with 10 software accumulations for each measurement. A 600 line/mm grating, laser source with 785 nm radiation, 200 μm pinhole aperture and a spectral range from 10 to 1600 cm^{-1} were used.

The N_2 adsorption and desorption isotherms were recorded at 77 K using a Quantachrome Nova 2200 Multi-Station High-Speed Gas Sorption Analyser after degassing of the samples at room temperature for 5 h in the degas station. Adsorbed nitrogen volumes were normalized to the standard temperature and pressure. The specific surface area (S_{BET}) was calculated according to the standard BET method in the relative absorption pressure (P/P_0) range from 0.045 to 0.250.

A Q5000 IR apparatus (TA Instruments) was used for thermogravimetric measurements under inert nitrogen atmosphere conditions, which were carried out over a temperature range of 25 to 800 °C with a scanning rate of 20°/min.

XPS measurements were obtained with a PHI5000 VersaProbe II (ULVAC-PHI, Chigasaki, Japan) operating with an aluminium monochromatic source ($\text{Al-K}\alpha = 1486.7\text{eV}$); data were collected by a hemispherical analyser operating in FAT mode. The analysis spot has a diameter of $100\ \mu\text{m}$ and a power of 25 W. The spectra from which the relative abundances were derived, were collected in the range $1100.0\text{-}0.0\ \text{eV}$ with a resolution (in energy) of $1.000\ \text{eV}$, for a time of about 3 minutes of illumination, at a pass energy (PE) of $117.400\ \text{eV}$.

A Bruker EMXmicro spectrometer was used for the EPR measurements. A dewar flask sample holder was used to perform the measurements at a temperature of 77 K using liquid nitrogen. Spectra were acquired from 0 to 800 mT with an attenuation of 12 dB (corresponding to a microwave power of 13.67 mW) and a gain 1×10^3 to obtain a good signal-to-noise ratio.

3. Experimental Results

The first aspect to be investigated was the crystallinity of ZIF-8 after the treatments. Figure 1 shows the diffractograms obtained for untreated ZIF-8 and for the samples belonging to the two sets, dried at room temperature and in an oven at $70\ ^\circ\text{C}$, treated at the different concentrations of copper in solution.

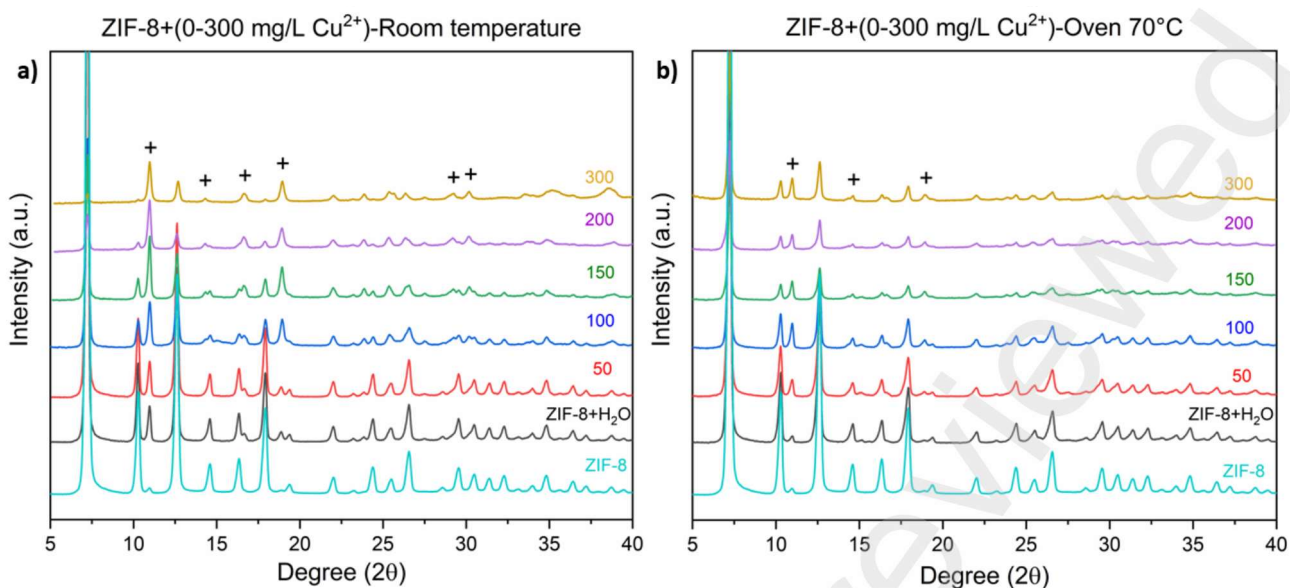


Fig.1: XRD patterns of ZIF-8 before and after immersion to aqueous copper solution with initial concentrations from 0 to 300 mg/L, for the set of samples dried at RT (a) and 70 °C (b); the '+' symbols indicate the characteristic peaks of the unknown phase formed by the effect of water alone.

After water exposure the XRD pattern of ZIF-8 shows a new peak at 16° that is related to a new and unknown crystalline phase reported by Zhang *et al.*^{14,15} caused by the hydrolysis of Zn^{2+} and 2-MeIm bonds. After treatments with copper a decrease in the intensity of ZIF-8 diffraction peaks and an increase of the peaks related to the unknown crystalline phase is observed as copper concentration rise. These effects are more evident for the set of samples dried at room temperature with respect to the set dried at 70 °C. It has been ruled out that the unknown crystalline phase does not belong to ZnO or any known complexes of 2-methylimidazole and zinc.

Raman measurements were performed on untreated ZIF-8 and after treatments with water and copper water solutions and the results are reported in Figure 2.

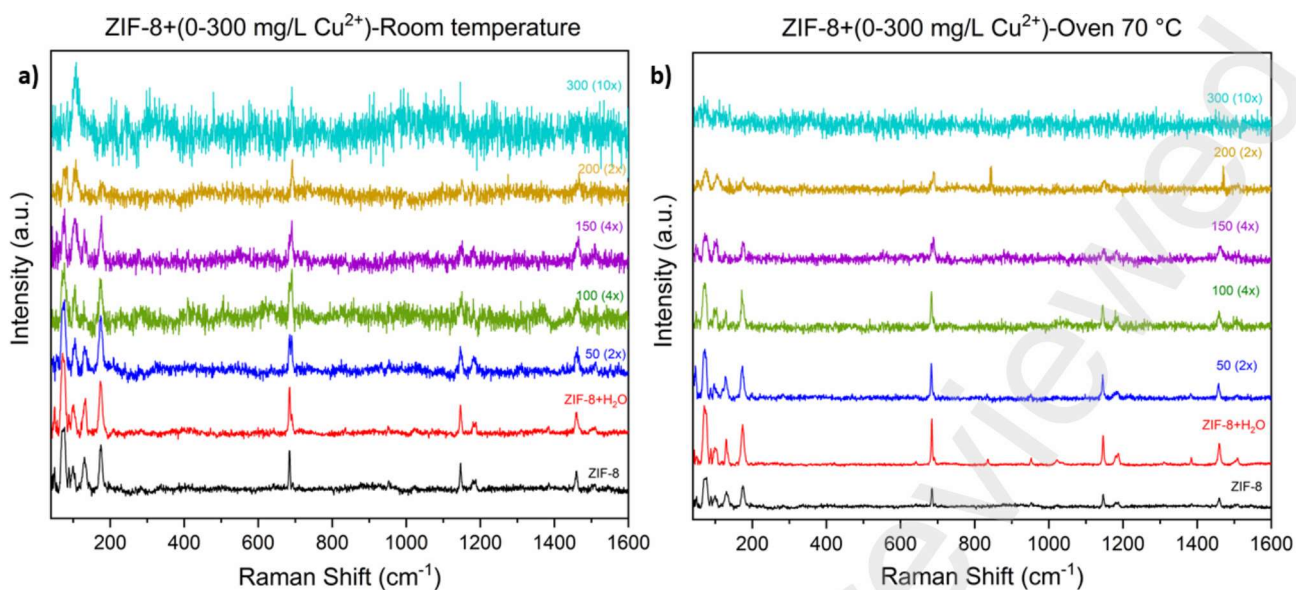


Fig. 2: Raman spectra of ZIF-8 before and after immersion to the aqueous copper solutions, for the set dried at RT (a) and for the set at 70 °C in the oven (b).

Raman spectra show some of the characteristic vibration of ZIF-8 like 173 cm^{-1} , 685 cm^{-1} , 1145 cm^{-1} and 1460 cm^{-1} corresponding to Zn–N stretching, imidazole ring puckering, C–N stretching and methyl bending, respectively²⁴. Moreover, Raman spectra show a clear decrease in signal amplitude as the copper concentration in solution increases. Although the XRD data give an indication of the formation of a new crystalline phase, no new peaks are observed in the Raman spectra. The absence of Raman signal in the new material suggests that its modification strongly affects the Raman scattering probability. A very significant aspect of the spectra shown in Fig. 2 is the Raman peak at 685 cm^{-1} , assigned in the literature to the puckering vibration of the imidazolate ring²⁴. An enlargement of the area around this peak is shown in Figure 3.

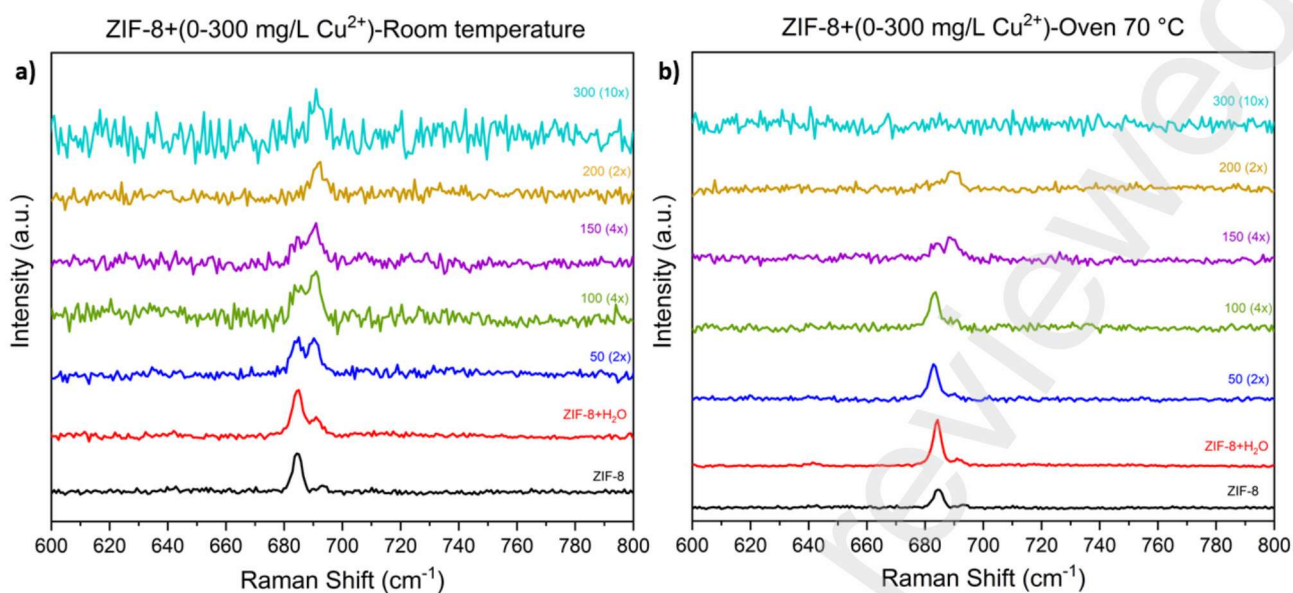


Fig. 3: Enlargement of Raman spectra for samples dried at RT (a) and those dried at 70 °C (b).

This specific Raman band undergoes splitting probably due to the protonation of a nitrogen atom of the imidazolate involved in a hydrolysis reaction due to the interaction of ZIF-8 with water. This hypothesis is supported by two elements: splitting already occurs for the sample treated only with water; splitting of the peak in two is much more pronounced for samples dried at room temperature than for those treated in an oven. Moreover, the relative intensity of the new peak adjacent to the characteristic peak of ZIF-8 increases as the copper concentration in solution to which the sample is exposed increases.

Porosimetry measurements were performed to assess the changes in surface area undergone by ZIF-8 following the various treatments. Figure 4 shows the surface area values of the set of samples dried in the dryer at room temperature and those of the set of samples dried in the oven.

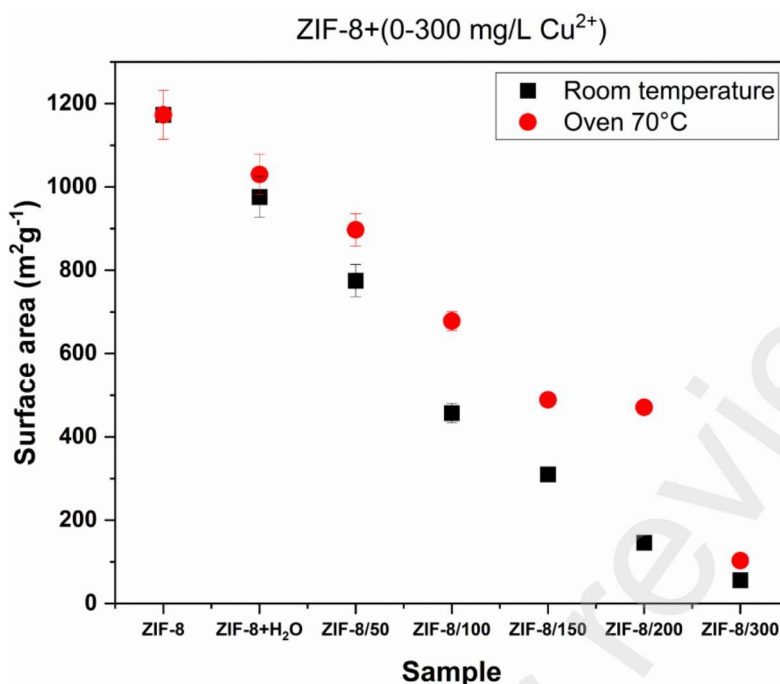


Fig. 4: Surface area (S_{BET}) of ZIF-8 of each sample treated with different concentrations of copper in aqueous solution (0-300mg/L), for the set dried at RT (black) and 70 °C (red).

Untreated ZIF-8 shows a BET surface area (S_{BET}) of $1173 \text{ m}^2 \text{ g}^{-1}$ that is in accordance with the typical values reported for this material^{25,26,27}. The S_{BET} of samples decreases with the water immersion and more increasing the copper concentration. As observed in the XRD and Raman data, these effects are more evident for the set of samples dried at room temperature with respect to the set dried at 70 °C. This finding is due to the presence of the unknown phase, which block the accessibility of the microporous structure, as observed by Zhang *et al.*^{17,18}.

TGA measurements were acquired for untreated ZIF-8 and after the treatments with copper solutions. In Figure 5 TGA of untreated ZIF-8, ZIF-8 treated with only water and treated with 150mg/L of Cu^{2+} aqueous solution are reported.

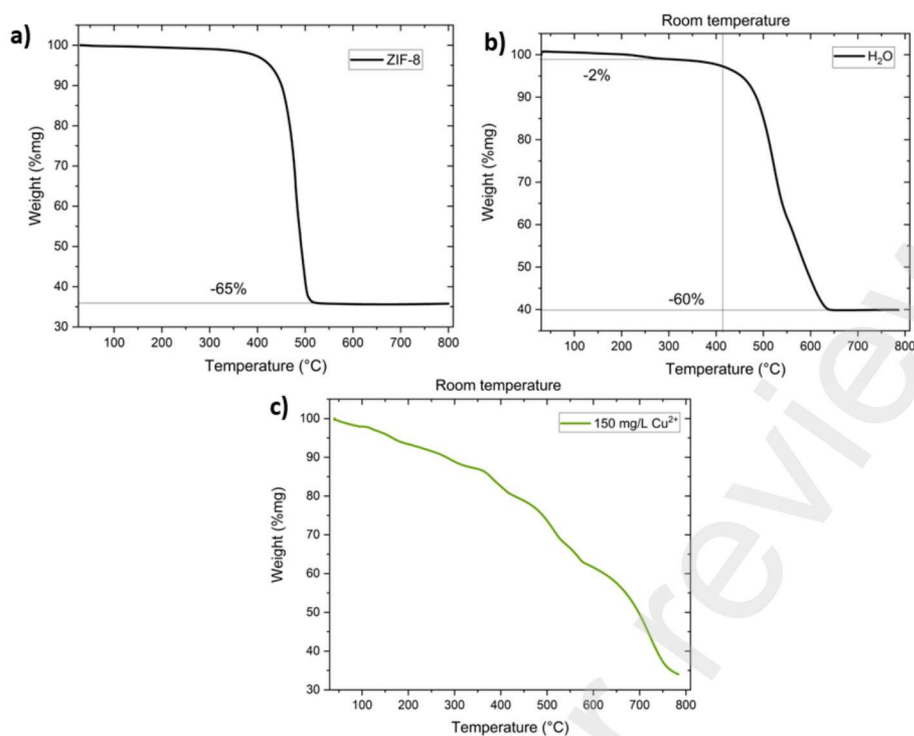


Fig. 5: TGA curve obtained for untreated ZIF-8 (a), ZIF-8 treated with only water (b) and treated with 150mg/L of Cu^{2+} aqueous solution (c).

TGA data for ZIF-8 shows a very big mass loss at 450 °C that is in accordance with the characteristic decomposition temperature for this material as previously reported in literature²¹⁻²³. Complete decomposition of ZIF-8 occurs at temperatures above 500 °C. In Figure S1 and Figure S2 TGA curves for ZIF-8 treated with copper aqueous solutions for both sets of samples are reported. TGA curves for these samples show a significant increase in complexity as the Cu^{2+} concentration in solution increases. Different new characteristic decomposition temperatures are observable suggesting the inhomogeneity of the recovered material. These effects are more prominent for the set of samples dried at room temperature.

XPS was performed for both set of samples and they are reported in Figure S3 and S4. The measurements confirmed that the copper present in the material recovered after the treatments is in the 2+ oxidation state for all samples, thus excluding any possible reaction of reduction. Given the relative abundances of the elements present, it was possible to calculate the Cu^{2+} content per unit

mass of material in the final structure. In the graph in Figure 6, these quantities are shown as a function of the Cu^{2+} concentration in solution.

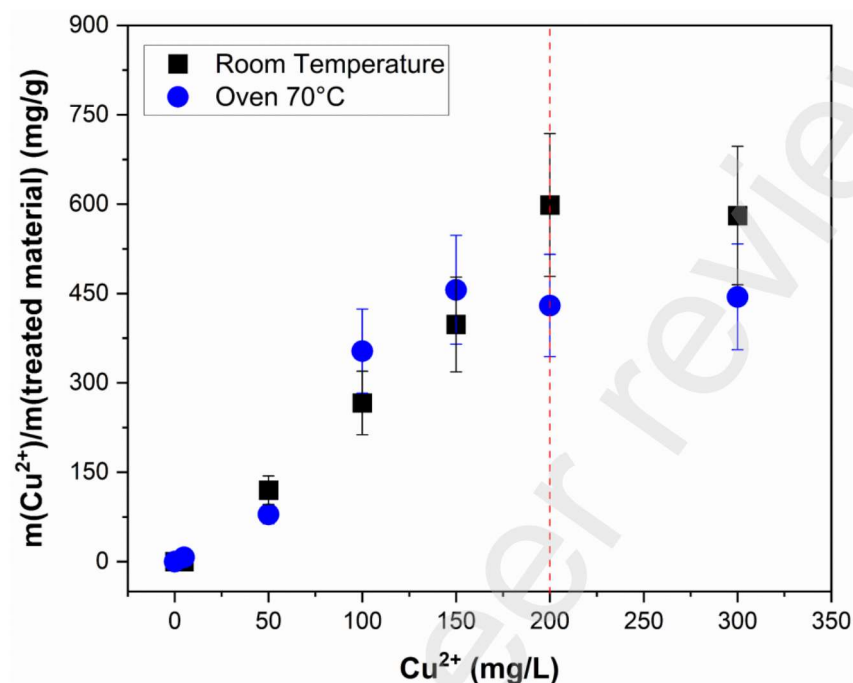


Fig. 6: Estimation of the amount of Cu^{2+} in the sample recovered as a function of the initial concentration of copper in solution, for the sample set dried at RT (in black) and for the set dried at 70°C (in blue).

The analysis carried out on the data established that the amount of copper captured by the material increases linearly with the Cu^{2+} concentration in solution, up to the threshold value of 200 mg/L, above which a constant saturation value is reached. This trend is observed for both sample sets and the value of copper captured in the final material is compatible within the experimental uncertainty for the two sets. Moreover, Figure S5 show the relative abundance of Zn^{2+} respect to untreated ZIF-8 (S5a) and O respect to C (S5b) for both sets of samples. It is possible to notice that the quantity of Zn^{2+} remain nearly constant suggesting that no ionic exchange between copper and zinc happen, while the quantity of oxygen rises as the concentration of copper increase suggesting that copper and oxygen may be bonded in the recovered material.

EPR spectra were acquired for both sets of samples with the scope to identify where copper ions are located in the structure of the recovered material. In Figure S6 and Figure S7 are reported experimental EPR spectra, fits and spectrum components obtained through the analysis for samples exposed to concentrations of 100 and 300 mg/L of copper of both prepared sets. These two cases were chosen to be presented as they are representative of the samples before and after the critical threshold of 200 mg/L.

EPR obtained for the samples after treatment show considerable complexity, probably due to the superposition of several lines belonging to different paramagnetic centres. It was possible to conclude from the fits performed that the experimental EPR spectra result from the partial superposition of three contributions from three different paramagnetic centres. One contribution, as expected, can be traced back to the Cu^{2+} ion in an octahedral configuration with a pronounced axial symmetry²⁸. The other two contributions are EPR rows traceable to $S=1/2$ spin centres (without any obvious hyperfine interaction), centred at lower magnetic field values, thus, traceable to hole centres and probably consisting of structures involving unbound oxygen atoms.

From the double integral of the EPR line associated with the Cu^{2+} ions, it is possible to obtain an estimate of the concentration of the paramagnetic centres. From this estimation, it is possible to determine the mass of copper captured per gram of final material obtained from the treatment. In Figure 7 it is showed the trend of this ratio as a function of copper concentration and compared it with that obtained from XPS measurements, for both sets of samples.

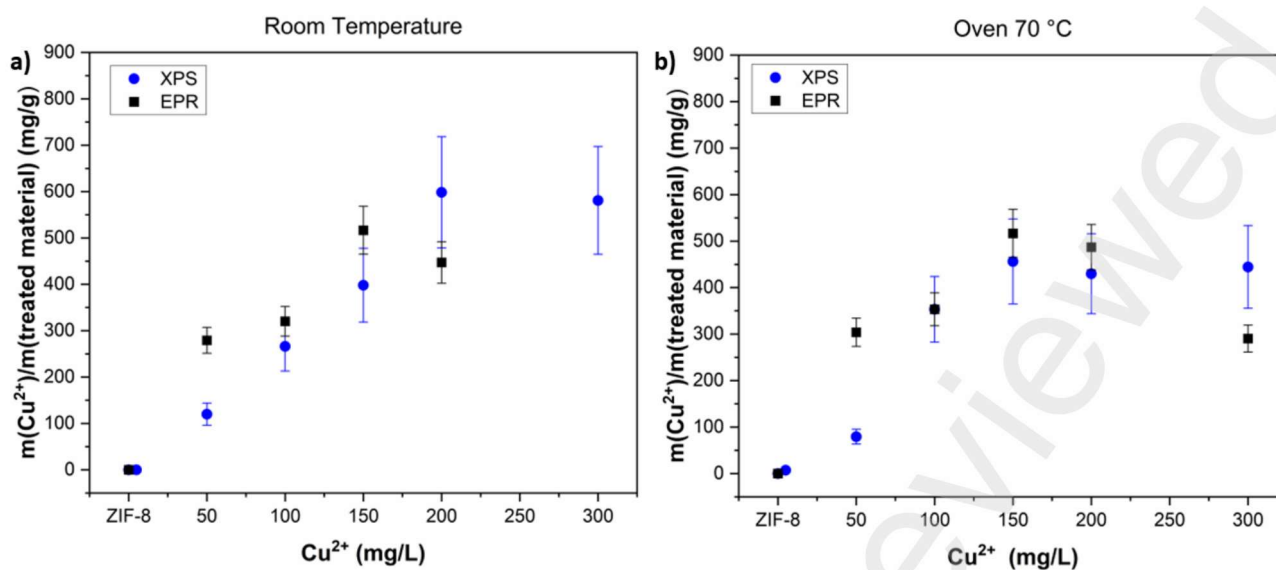


Fig. 7: Comparison of XPS (blue circles) and EPR (black squares) estimates of the copper content per unit mass of the final material, for the set of samples dried at RT (a) and for the set dried at 70°C (b).

From the data shown in Fig. 7 the quantity of copper estimated by XPS and EPR are in excellent agreement with each other within the experimental error.

4. Discussions

The data obtained from XRD, Raman, BET and TGA for the ZIF-8 treated with copper aqueous solutions, clearly show two main results. The first one is that water affect the crystalline structure resulting in the formation of a new unknown crystalline phase, as shown by XRD, which is also non porous and resulting in the lowering of surface area. Considering that the ZIF-8/water weight ratio used in these experiments was 0.1 wt.%, these results are in perfect agreement with what Zheng *et al.*^{13,14} have previously reported confirming that when ZIF-8 is dispersed in water solutions, with a ZIF-8/water weight ratio of 6.0 wt.% or lower the material crystalline structure undergoes a hydrolysis reaction that leads to the formation of this new crystalline material. The second result is related to effects induced by Cu²⁺ in water solution. Indeed, copper ions dramatically promote the

decomposition of ZIF-8 structure. As the concentration of copper increases the presence of the new crystalline phase rise as confirmed by XRD and Raman and a progressive reduction of the surface area is simultaneously observed. The resulting recovered product is inhomogeneous as can be seen by TGA measurement where new different characteristics decomposition temperatures appear. This effect appears to be limited up to a concentration of 50 mg/L, at which plausibly ZIF-8 appears to tolerate the amount of copper in solution, or in any case the decomposition process is marginal compared to those induced by the interaction with water. In addition, it is evident that the effects induced by the immersion of the material into water and copper ions solutions is generally much more pronounced for the sample set dried at room temperature than for the one dried in oven. This is probably due to the longer drying time required for the former set compared to the latter, which results in the sample being exposed to the aqueous copper solution for a longer time, favouring the dissolution process.

Regarding the copper capture process XPS and EPR gives important information helping to clarify the mechanism of capture. These measures showed that the amount of copper captured rises linearly till a threshold concentration of 200 mg/L in aqueous solution that corresponds to 600 mg g⁻¹ of copper capture capacity. This value, despite the decomposition process which ZIF-8 undergo, is above any other adsorbent system for copper, for which lower values are obtained even by an order of magnitude²⁹ and are in agreement with what was reported by Zhang *et al.*¹⁸ Our result is surprising considering that in the above study it is declared that the capture takes place through ion exchange, while in our study it is evident that under the experimental conditions considered, ZIF-8 in aqueous copper solution decomposes and partially reorganizes into a new structure. Our results could be very promising in principle, but this is not actually true. In fact, in real applications the ZIF-8/water mass ratio would be much lower than the 0.1 wt.% value considered in the experiments carried out in this study, resulting in a more pronounced decomposition of the material. Furthermore, the formation of a solid component containing copper captured from the solution begins only when the concentration of Zn and imidazolate ions exceeds a certain threshold value. Due to the low value of ZIF-8 /water

mass ratio, this value would never be reached in real applications and rather the complete dissolution of ZIF-8 would occur. Consequently, not only would the copper remain in the solution, but also other components not previously present will be introduced, such as Zn ions and imidazolate, thus polluting further. Finally, the high economic cost of this material and the problem of recovering it after the treatment makes the use of ZIF-8 even less practical: in the real case it would be expensive and complex to operate the water filtering in a similar way to that performed in the laboratory. The dissolution of the ZIF-8 and the difficulty of recovering the final material would lead to a type of pollution, due to the cleaning systems used, called *secondary pollution*^{30,31}.

Concerning the capture mechanism this study demonstrates that ionic exchange is not primary because, as shown by relative abundance of Zn²⁺ and O²⁻ obtained from XPS data, the amount of zinc remains constant as the amount of captured copper rises, while the amount of oxygen rises too. This suggests that copper does not substitute zinc but probably it is bounded to oxygen. In addition to this, EPR spectra suggest that copper is bounded in an octahedral configuration to oxygen but is not possible to exclude also to nitrogen because in EPR the two interactions are virtually indistinguishable.

5. Conclusions

In Summary, here we have reported a study on the stability of ZIF-8 as sequestering agent for copper ions in aqueous solutions, the efficiency of this process and the kind of capture mechanism. Our results point out that ZIF-8 crystalline structure, when dispersed in water at pH=7 and with a ZIF-8/water mass ratio of 0.1 wt.%, undergoes a hydrolysis reaction caused by water that result in the decomposition of ZIF-8 and a reorganization in a new unknown crystalline non porous material. Furthermore, Cu²⁺ in water promotes this decomposition, but copper ions are bonded in the new crystalline structure resulting in an efficient capture with a maximum value of 600 mg g⁻¹ of captured copper ions that is higher than any other reported material for copper sequestration. However, the

high cost, the difficulty in recovering the material after immersion into the copper solution and the decomposition effects that can cause secondary pollution, make ZIF-8 not suitable for practical use at least in simply powder form. As the concentration of copper in solution increased, and therefore copper in the final material, relative abundance of zinc remains constant for all samples obtained, suggesting that the copper adsorption process did not occur by ion exchange, as previously suggested in the literature. Furthermore, XPS data indicate that the amount of oxygen present in the samples increases with increasing copper content. This information, together with EPR data identifying copper in octahedral configuration, suggests that the ion coordinates with oxygen and probably also nitrogen atoms in the structure of the final material.

6. References

1. S. Bolisetty, M. Peydayesh and R. Mezzenga, *Chem. Soc. Rev*, 2019, **48**, 463–487.
2. D. Briggs, *Br. Med. Bull.*, 2003, **68**, 1–24.
3. S. A. Alrumman, A. F. El-kott and S. M. A. S. Keshk, *Am. J. Environ. Eng*, 2016, **6**, 88-98.
4. J. Singh, P. Yadav, A. K. Pal, and V. Mishra, in *Sensors in Water Pollutants Monitoring: Role of Material*, ed. D. Pooja, P. Kumar, P. Singh, S. Patil, Springer Singapore, Singapore, 1, 2020, Water Pollutants: Origin and Status, 5-20.
5. N. Shaheen, Md. K. Ahmed, Md. S. Islam, Md. Habibullah-Al-Mamun, A. B. Tukun, A. T. M. A. Rahim, *Environ. Sci. Pollut. Res.*, 2016, **23**, 7794–7806.
6. Institute of Medicine (US) Panel on Micronutrients. Dietary Reference Intakes for Vitamin A, Vitamin K, Arsenic, Boron, Chromium, Copper, Iodine, Iron, Manganese, Molybdenum, Nickel, Silicon, Vanadium, and Zinc. Washington (DC): National Academies Press (US); 2001
7. Guidelines for Drinking-Water Quality: Fourth Edition Incorporating the First Addendum. Geneva: World Health Organization; 2017. PMID: 28759192.
8. R. Squitti, M. Siotto and R. Polimanti, *Neurobiol. Aging*, 2014, **35**, S40-S50.
9. A. La Torre, V. Iovino and F. Caradonia, *Phytopathol. Mediterr.*, 2018, **57**, 201–236.

-
10. L. Tamm, B. Thuerig, S. Apostolov, H. Blogg, E. Borgo, P. E. Corneo, S. Fittje, M. de Palma, A. Donko, C. Experton, E. Alcázar Marín, Á. Morell Pérez, I. Pertot, A. Rasmussen, H. Steinshamn, A. Vetemaa, H. Willer and J. Herforth-Rahmé, *Agronomy*, 2022, **12**, 673.
11. K. Rehman, F. Fatima, I. Waheed and M. S. H. Akash, *J. Cell. Biochem*, 2018, **119**, 157-184.
12. A.A Taylor, J.S. Tsuji, M.R. Garry, M.E. McArdle, W. L. Goodfellow Jr, W. J. Adams and C. A. Menzie, *Enviro. Manage.* 2020, **65**, 131–159.
13. H. C. Zhou, J. R. Long and O. M. Yaghi, *Chem. Rev.*, 2012, **112**, 673-674.
14. M. Feng, P. Zhang, H. C. Zhou and V. K. Sharma, *Chemosphere*, 2018, **209**, 783-800.
15. P. A. Kobielska, A. J. Howarth, O. K. Farha and S. Nayak, *Coord. Chem. Rev.*, 2018, **358**, 92–107.
16. K. S. Park, Z. Ni, A. P. Côté, J. Y. Choi, R. Huang, F. J. Uribe-Romo, H. K. Chae, M. O'Keeffe and O. M. Yaghi, *Proc. Nat.l Acad. Sci. U S A.*, 2006, **103**, 10186-10191.
17. H. Zhang, M. Zhao and Y. S. Lin, *Microporous Mesoporous Mater.*, 2018, **279**, 201–210.
18. H. Zhang, M. Zhao, Y. Yang and Y. S. Lin, *Microporous and Mesoporous Mater.*, 2019, **288**, 109568.
19. P. A. Kobielska, A. J. Howarth, O. K. Farha and S. Nayak, *Coord. Chem. Rev.*, 2018, **358**, 92–107.
20. A. Tanihara, K. Kikuchi and H. Konno, *Inorg. Chem. Commun.*, 2021, **131**, 108782.
21. K. Li, N. Miwornunyuie, L. Chen, H. Jingyu, P. S. Amaniampong, D. Ato Koomson, D. Ewusi-Mensah, W. Xue, G. Li and H. Lu, *Sustainability*, 2021, **13**, 984.
22. Y. Zhang, Z. Xie, Z. Wang, X. Feng, Y. Wang and A. Wu, *Dalton Trans.*, 2016, **45**, 12653-12660.
23. L. Zhang and Y. H. Hu, *J. Phys. Chem. C*, 2011, **115**, 7967–7971.
24. G. Kumari, K. Jayaramulu, T. K. Maji and C. Narayana, *J. Phys. Chem. A*, 2013, **117**, 11006–11012.
25. N. A.H. M. Nordin, A. F. Ismail, A. Mustafa, M. Surya Murali and T. Matsuura, *RSC Adv.* 2014, **4**, 52530-52541.
26. A. Almasoudia and R. Mokaya, *J. Mater. Chem.*, 2012, **22**, 146-152.
27. R. P. P. L. Ribeiro, C. L. Antunes, A. U. Garate, A. F. Portela, M. G. Plaza, J. P. B. Mota and I. A. A. C. Esteves, *Microporous and Mesoporous Mater.*, 2019, **275**, 111-121.
28. M. Todaro, G. Buscarino, L. Sciortino, A. Alessi, F. Messina, M. Taddei, M. Ranocchiari, M. Cannas and F. M. Gelardi, *J. Phys. Chem. C*, 2016, **120**, 12879-12889.

29. V. Krstić, T. Urošević and B. Pešovski, *Chem. Eng. Sci.*, 2018, **192**, 273–287.

30. H. Md Anawar and R. Chowdhury, *Sustainability*, 2020, **12**, 7017.

31. F. Lu and D. Astruc, *Coord. Chem. Rev.*, 2020, **408**, 213180.